Journal of Nuclear Science and Technology

ISSN: 0022-3131 (Print) 1881-1248 (Online) Journal homepage: https://www.tandfonline.com/loi/tnst20

Characteristics of Counter current Gas-Liquid Two-Phase Flow in Vertical Tubes

Katsuji YAMAGUCHI & Yasaburo YAMAZAKI

To cite this article: Katsuji YAMAGUCHI & Yasaburo YAMAZAKI (1982) Characteristics of Counter current Gas-Liquid Two-Phase Flow in Vertical Tubes, Journal of Nuclear Science and Technology, 19:12, 985-996, DOI: 10.1080/18811248.1982.9734247

To link to this article: https://doi.org/10.1080/18811248.1982.9734247

Published online: 15 Mar 2012.

Characteristics of Countercurrent Gas-Liquid Two-Phase Flow in Vertical Tubes

Katsuji YAMAGUCHI,

*Ship Research Institute**

Yasaburo YAMAZAKI†

*Japan Atomic Energy Research Institute***

Received January 8, 1982
Revised July 9, 1982

Investigations into the flow pattern and the void fraction for countercurrent air-water flow in vertical tubes of diameter D=40 and 80 mm were reported. The flow maps were presented and showed slug flow regime occupied larger portion on them. The void fraction was measured by the quick-closing valve technique, in bubbly and slug flow regime.

The void fraction data available in the literatures as well as present work for countercurrent flow in vertical tubes were correlated in terms of dimensionless groups. The experimental results of the present work were also compared with the drift flux model.

KEYWORDS: two phase flow, upflow, downflow, countercurrent flow, flow pattern, flow regime map, bubbly flow, slug flow, void fraction correlation, drift flux model

I. INTRODUCTION

Countercurrent two-phase flow through a vertical channel (gas phase flows upward and liquid phase flows downward) occurs in nuclear reactors during the analysis of a Loss-of-Coolant Accident (LOCA), in chemical equipments and in thermosyphons. Because of the difference between various flow operations such as upflow, downflow and countercurrent flow, thermal and hydraulic characteristics have been investigated for each flow operation.

Studies on the critical heat flux (CHF) for countercurrent flow have been made by Griffith *et al.*[1] They used the CHF *vs.* void fraction curve to predict CHF. Proposal to describe the state of the system was done by using void fraction rather than quality. The void fraction was measured at very restricted gas and liquid velocities by Shulman & Molstad[2], Bridge *et al.*[3], Fantini *et al.*[4] and Mochan *et al.*[5][22] The bubble velocity in slug flow for countercurrent flow was measured by many investigators[6]~[11]. Some of the researchers succeeded to correlate the limited number of experimental data with the drift flux model but at very narrow experimental conditions. Unfortunately, the correlations found in the literatures[4][11][20] are applicable only to a certain type of flow pattern and a limited range of operating conditions. To date there have been no flow regime map for countercurrent flow.

This paper presents flow regime maps and a generalized correlation of the void fraction in bubbly and slug flow regime for countercurrent two-phase flow in vertical tubes.

---

* *Shinkawa, Mitaka-shi, Tokyo 181.*
** *Tokai-mura, Ibaraki-ken 319-11.*
† Present address: Faculty of Engineering, Tokai University, *Tomigaya, Shibuya-ku, Tokyo 151.*

II. Experimental Equipment and Procedures

Experiments were carried out on the two different equipments for the countercurrent flow of air-water mixtures having 40 and 80 mm I.D. vertical plexiglass tubes. The experimental procedures were almost the same for these two equipments.

A schematic flow sheet of the equipment for the 40 mm diameter tube is shown in **Fig. 1** (the equipment of an 80 mm tube is very similar). The test section consisted of a circular vertical tube with quick-closing valves and a static pressure tap. Water was supplied to the upper tank ⑦ and then flowed down by gravity into the test section ① by overflowing over a circular weir. A constant water level was kept in the upper tank. Water flow was controlled by the glove valve ③ and was measured by rotameter ④ when it was discharged to the lower tank ⑤. Air was fed to mixing chamber ② from a compressor ⑧. After rising through the test section, air was vented to the atmosphere. The mixing method has effect on flow behaviors. A tapered end design which gives reproducible measurements was adopted[12]. A detail of the mixing chamber of a 40 mm tube is shown in **Fig. 2.** Air was injected through a porous bronze plate with equal diameter to the inside diameter of the test section and with a hole size of approximately 40 μm. Air flow rate was measured by the rotameter ⑨ before being fed to the mixing chamber.

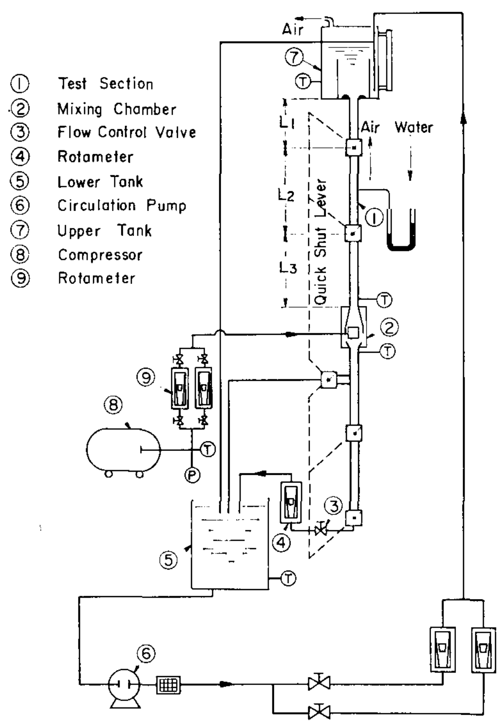

Fig. 1 Schematic diagram of experimental equipment

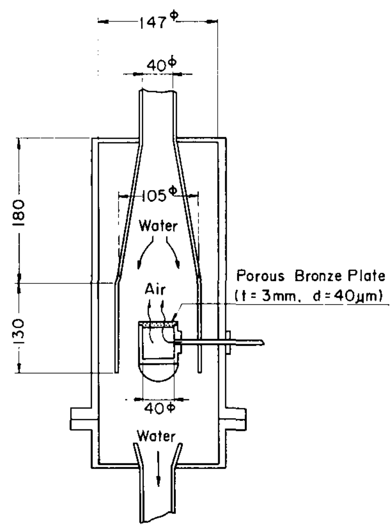

Fig. 2 Mixing chamber

Void fraction was measured with increasing the water flow for constant air flow. In the slug flow regime there were fluctuations in flow rate, especially in the water flow rate. These fluctuations occur due to the variations of the average fluid density and pressure loss in the test section. The averaged readings of rotameter were used.

The dimensions of the test sections are summarized in **Table 1.**

The void fraction was measured by means of quick-closing valve technique. The velocity of the bubbles in the slug flow regime was determined by a stopwatch. The range of variables covered in these tests is listed in **Table 2.** Upward direction is taken positive in this table and throughout this paper. The temperature in all the experiments was 20±5°C.

Table 1 Dimension of test section

D(mm)	L_1(cm)	L_2(cm)	L_3(cm)
80	160	170	160
40	70	80	100

Table 2 Range of variables covered in experimental tests (void fraction)

D (mm)	$\langle j_g \rangle$ (cm/s)	$-\langle j_l \rangle$ (cm/s)
80	0.68~106	0~35.4
40	0.68~115	0~22.7

III. Experimental Results

1. Flow Pattern

All published literatures(2)(3)(8)(9)(11) on flow behaviors in countercurrent flow are restricted studies to a limited region within each flow pattern. The following flow behaviors for the entire flow pattern were observed, in general, as the gas flow rate was increased for constant liquid flow. The determination of flow pattern was made by visual observations and photographic techniques.

At small air flow rate bubbles are apparently not interacted and seem to be characterized by uniform distribution and uniform velocity throughout the tube. This flow is designated as flow pattern of type I. As the gas flow rate is increased, bubbles tend to generate wakes and to rise at uneven velocity. The path of the gross motion of the bubbles oscillates (flow pattern of type II). Then, wake flow becomes turbulent, large nonspherical bubbles of different size appear (flow pattern of type III). Similar flow behaviors for three kinds of flow pattern in bubbly flow were also observed by Zuber *et al.*(23) for bubbling experiment. As the gas flow rate is further increased large bubbles which has irregularly shaped nose and are occupied nearly entire cross-sectional area of tube are formed(9)(11). It was found small bubbles in the liquid slugs following the large bubble. Then, the interface between the two phases is violently agitated and the length of bubble slug is increased. The liquid film around the bubble slug seems considerably thick, flowing down with small bubbles in it (slug flow, flow pattern of type IV). **Photograph 1** shows typical flow patterns. After that flow pattern changes to annular

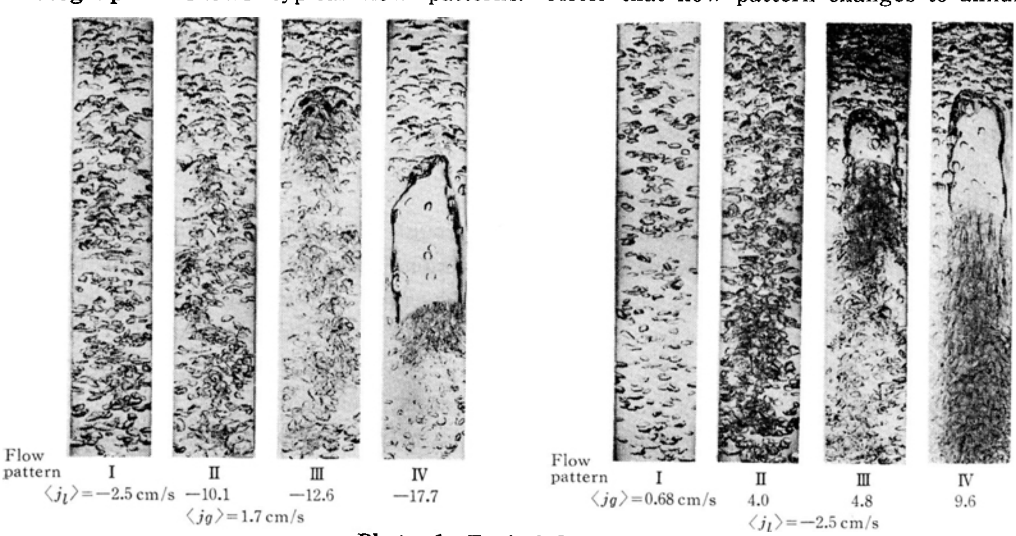

Photo. 1 Typical flow patterns

flow and flow attains the flooding which corresponds to the limit of the countercurrent flow.

Figures 3(a) and (b) show observed flow patterns such as bubbly, slug and annular flows which are plotted on the maps at various flow rates. In these figures flow patterns of types I, II and III are grouped in the bubbly flow, where average diameter of bubble in the bubbly flow was 5∼6 mm. On the same figure for D=40 mm, also the values predicted by the equation of Wallis[16] for flooding were shown. It is noted that significant differences of the transition boundaries of the flow regimes exist between the upflow[18] and the countercurrent flow. For example, the transition from bubbly to slug flow occurs by decreasing the gas flow rate for countercurrent flow but by increasing the gas flow rate for upflow when increasing the absolute value of water flow rate.

For 40 mm diameter tube in countercurrent flow, the transition from slug to annular flow of single bubble corresponds to with zero volumetric flux density of air occurs at $\langle j_l \rangle \approx -20$ cm/s. In the experiment of downflow, Golan & Stenning[17] showed that this transition occurred at $\langle j_l \rangle = -20.3$ cm/s for a 1∼1.5 in. I. D. tube.

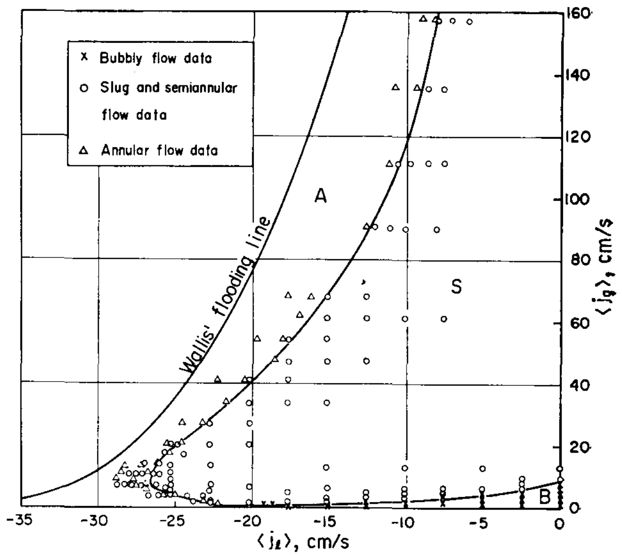

(a) D=40 mm

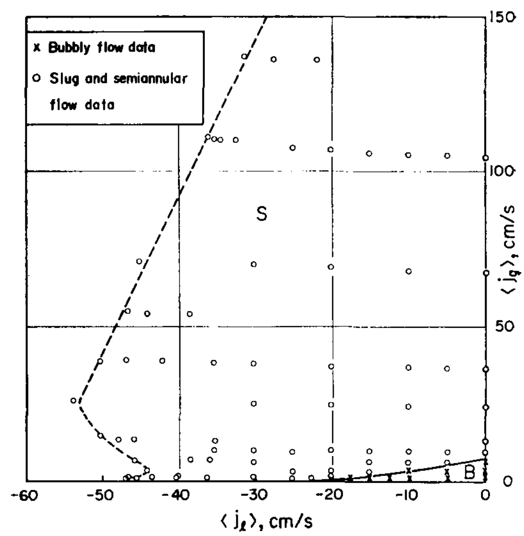

(b) D=80 mm

Fig. 3(a), (b) Flow regime map D=40 and 80 mm

The dashed line in Fig. 3(b) denotes the occurrence of considerable air escape through the liquid exit while the remaining of supplied air flows upward in the test section. Escaped air is the small bubbles following the bubble slug. This phenomenon was observed in the slug flow. Therefore, it was impossible to obtain the transition to annular flow with the apparatus of D=80 mm.

2. Void Fraction

In **Fig.** 4 the void fractions $\langle \alpha \rangle$ are plotted against volumetric flux density of gas $\langle j_g \rangle$ for various volumetric flux density of liquid $\langle j_l \rangle$, where × denotes the transition from bubbly to slug flow. It is seen that the $\langle \alpha \rangle$ increases with increasing $\langle j_g \rangle$. For the effects of $\langle j_l \rangle$, somewhat different trend was obtained between the experimental points of a diameter of 40 mm tube and the data of 80 mm tube. This is much more clearly seen

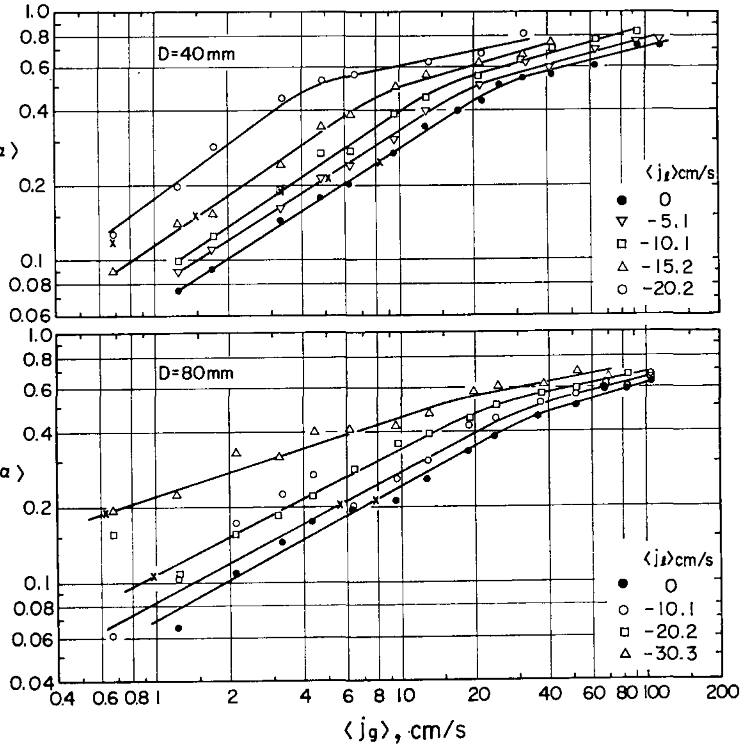

Fig. 4 Void fraction *vs.* volumetric flux density of gas

from **Fig. 5**, where the data are plotted for D=40 and 80 mm. The results show significant influence of tube diameter on void fraction. Due to the transition of flow regime during the variation of liquid velocity for constant air flow, void fraction for D=80 mm shows a complicated trend. It was observed that the void fraction values for 40 mm tube are larger than corresponding values of 80 mm tube for the same liquid and gas volumetric flux density at higher flux density. While the difference between the values of $\langle\alpha\rangle$ for different diameter decreases with decreasing the absolute value of volumetric flux density of the liquid and gas phases.

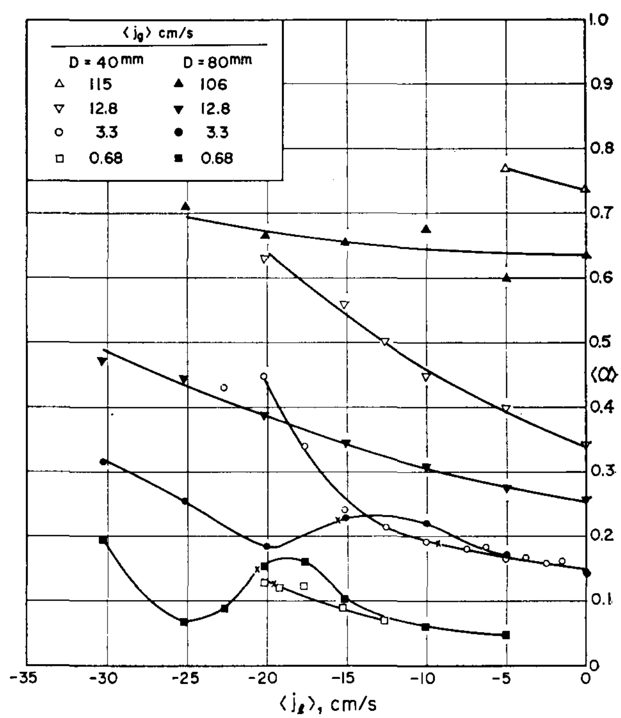

Symbol × denotes the transition point from bubbly to slug flow.

Fig. 5 Void fraction data for different diameter of test section

IV. Analysis of Results

1. Comparison of Void Fraction Data with Previously Reported Correlations

The experimental results obtained for countercurrent flow operation were examined to correlate with the drift flux model, which were proposed by Wallis[13] and Zuber & Findlay[14].

Wallis presents an equation of the form of

$$\langle j_{gl}\rangle=\langle j_g\rangle-\langle\alpha\rangle\langle j\rangle = v_\infty\langle\alpha\rangle(1-\langle\alpha\rangle)^k, \qquad (1)$$

where v_∞ is the terminal rise velocity of a single bubble in an infinite medium. The equation of Zuber & Findlay is

$$\frac{\langle j_g\rangle}{\langle\alpha\rangle}=C_0\langle j\rangle+V_{gj}, \qquad (2)$$

where coefficient C_0 depends on the flow distribution, V_{gj} is termed drift velocity.

Figure 6(a) shows the experimental results of the flow pattern of type I (see Sec. III-1) for 40 and 80 mm in diameter together with the data of Shulman & Molstad[2], Bridge *et al.*[3] and of Fantini *et al.*[4] for countercurrent air-water flow which are correlated according to Eq. (1) using

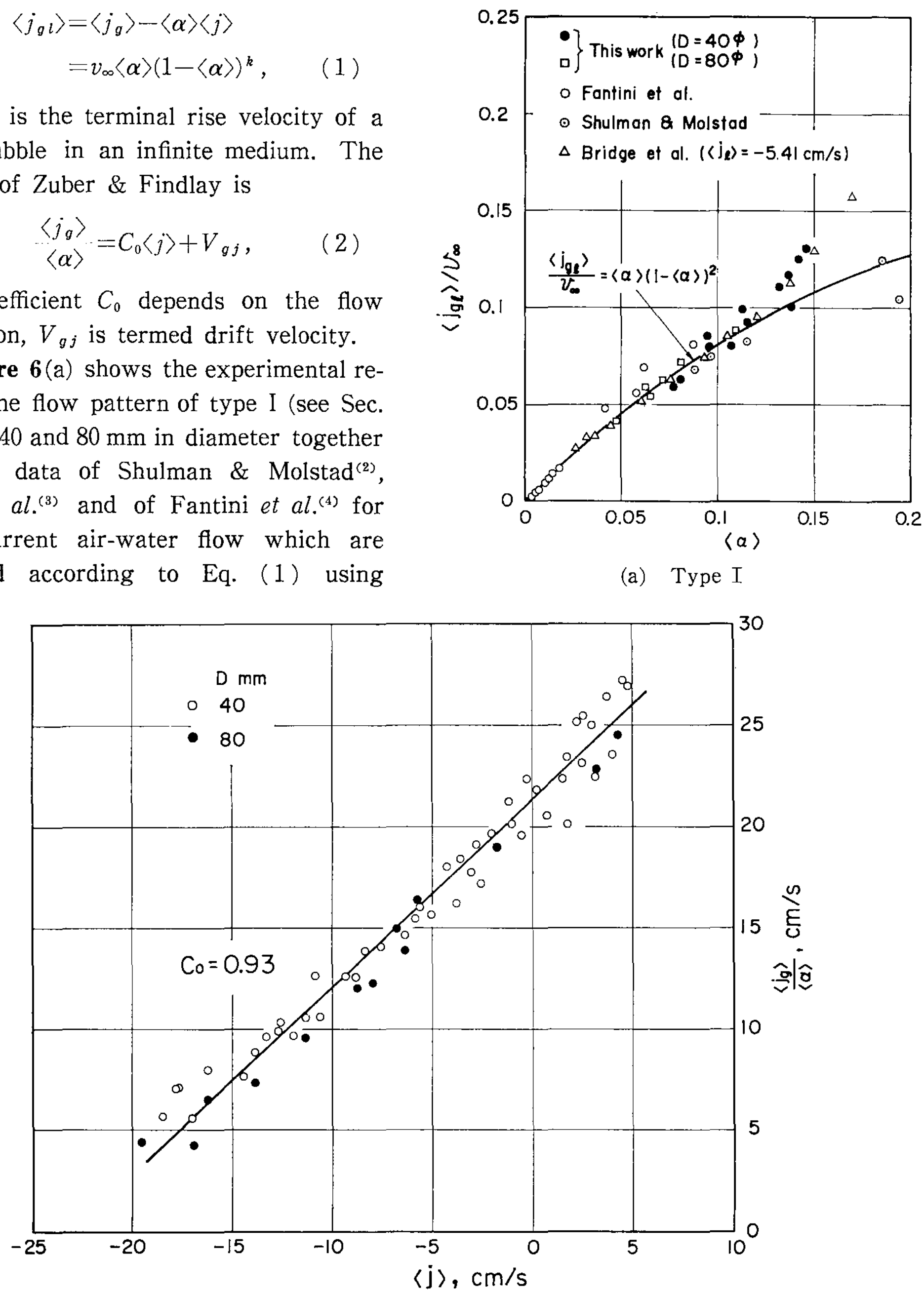

Fig. 6(a),(b) Void fraction of flow pattern of Type I, Types II and III

$k=2$, while v_∞ can be calculated using the experimental curve presented by Haberman & Morton[19]. The agreement between the equation and the experimental results is good for lower void fraction. This result agrees with the flow observation that the flow is one-dimensional for low velocities and low void fraction. The disagreement between the equation and the data for higher void fraction in this figure is probably due to the void fraction and velocity distributions.

The data of $\langle j_g \rangle / \langle \alpha \rangle$ and $\langle j \rangle$ for flow patterns of types II and III (see Sec. III-1) are plotted on Fig. 6(b) for $D=40$ and 80 mm. The data are insignificantly affected by tube diameter. From the straight line through the data the value of C_0 in Eq. (2) is $C_0=0.93$, which is not the same value as that of previous works[14][20][24] for cocurrent flow and $V_{gj}=v_\infty$, which is in agreement with the result for upflow.

The results of slug flow tests for $D=80$ mm are shown in **Fig. 7**. Apparently the effects of $\langle j_g \rangle$ are not seen in the figure. A very similar results obtained also for $D=40$ mm. For comparison, the values found in the literatures[9][21] of C_0 and V_{gj} in slug flow for upflow are also represented on the same figure. The slope of the straight line through the data seems to be approximately equal to $C_0=1.2$, however, the drift velocity is greater than $0.35\sqrt{gD}$. Measured velocities of bubble slugs for varying the flow rate of each phase and of a single slug generated in the tube at the given water flow rate are also compared with the solid line for $D=40$ mm in **Fig. 8**. The results show that the solid line disagrees with these velocities. Rather complicated variation of the velocity of the single slug for water velocity depends on the magnitude of the distortion and eccentricity of the bubble. For $D=80$ mm, the single slug becomes very unstable if the downward water flow is increased and for $\langle j_l \rangle \leq -44$ cm/s, bubble slug breaks up into small bubbles.

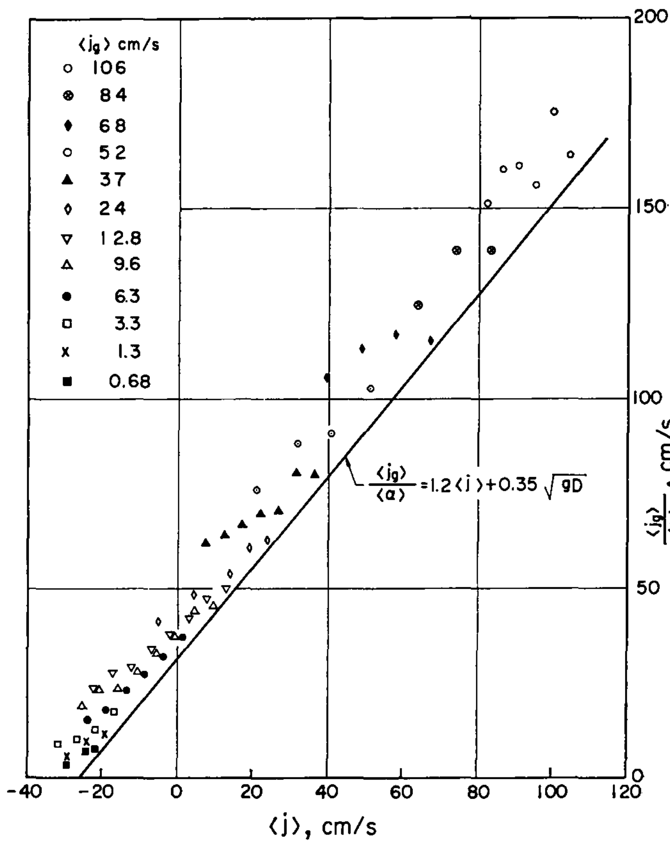

Fig. 7 Void fraction of slug flow ($D=80$ mm)

The drift flux model, the only established model which may be used for analyzing the countercurrent flow, was examined to correlate the void fraction data for countercurrent flow. This model seems to have a tendency to represent the experimental results for countercurrent flow. But at present time, it is difficult to determine the parameters in Eqs. (1) and (2) for wide operating countercurrent flow conditions. Therefore, another expression applicable to

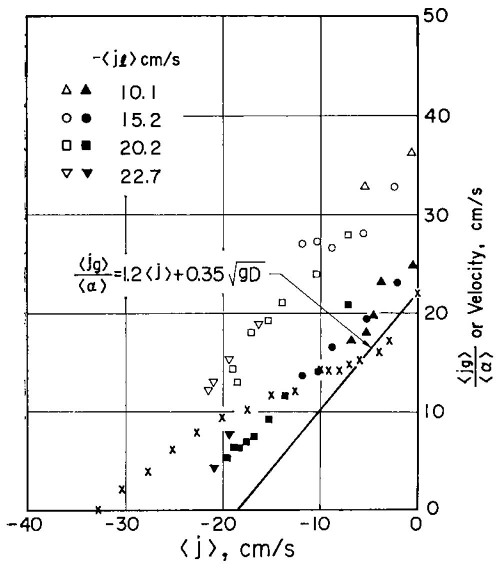

White symbols: Velocity of bubble slug measured by a stopwatch
Black symbols: Gas velocity calculated from void fraction ($\langle j_g\rangle/\langle\alpha\rangle$)
Symbol × denotes the velocity of a single bubble slug.

Fig. 8 Various velocities in slug flow (D=40 mm)

bubbly and slug flow regime for countercurrent flow in vertical tubes will be presented in the following sections.

2. Development of Void Fraction Correlation by Dimensionless Groups

(1) Dimensional Analysis

By assuming the void fraction $\langle\alpha\rangle$ is a function of the specific weights γ_l and γ_g, the viscosities μ_l and μ_g, the surface tension σ, tube diameter D, volumetric flux densities $\langle j_l\rangle$ and $\langle j_g\rangle$ for non-boiling two-phase flow in tubes, a functional relation between void fraction and dimensionless groups has been obtained by Sudo[15] through the dimensional analysis on these variables. The following relation, Eq. (3) which is very similar to his relation but introducing the quantity $\mu_l\langle j_g\rangle/\sigma$ instead of $\mu_g\langle j_g\rangle/\sigma$, will be used hereafter.

$$\langle\alpha\rangle=f(\gamma_g/\gamma_l,\ \mu_g/\mu_l,\ \mu_l\langle j_g\rangle/\sigma,\ \gamma D^2/\sigma,\ \langle j_g\rangle/\langle j_l\rangle)\,. \tag{3}$$

Thus, there are five dimensionless groups that may be used to predict the void fraction. Next the form of function f will be determined. Sudo[15] presented the following empirical correlation of the void fraction which can be applied to gas-water systems at very low volumetric flux density of water including the stagnant water condition

$$\langle\alpha_1\rangle=\text{const.}(\gamma_g/\gamma_l)^{m_1}(\mu_g/\mu_l)^{m_2}(\gamma_l D^2/\sigma)^{m_3}(\mu_l\langle j_g\rangle/\sigma)^{m_4}\,. \tag{4}$$

Denote $\langle\alpha\rangle=\langle\alpha_0\rangle$ for $\langle j_l\rangle=0$ keeping the other variables constant, then it may be expressed as

$$\langle\alpha_1\rangle\approx\langle\alpha_0\rangle\,. \tag{5}$$

Considering Eqs. (3), (4) and (5), the following expression is a possible form of the correlation of void fraction for countercurrent flow, *i.e.*

$$\frac{\langle\alpha\rangle}{\langle\alpha_0\rangle}=1+\text{const.}(\gamma_g/\gamma_l)^{n_1}(\mu_g/\mu_l)^{n_2}(\sqrt{\gamma_l D^2/\sigma})^{n_3}(\mu_l\langle j_g\rangle/\sigma)^{n_4}(-\langle j_l\rangle/\langle j_g\rangle)^{n_5}\,. \tag{6}$$

Equation (6) was attempted to correlate the experimental data available in the literatures for countercurrent flow in vertical tubes but there exist few experimental works. The data of $\langle\alpha\rangle/\langle\alpha_0\rangle$ were obtained from the experimental results of this work and Bridge *et al.*[3] for air-water flow system, Bridge *et al.*[3] for air-58% glycerine solution flow system ($\mu_l=7.99\times10^{-4}$ kg/m^2), and Mochan *et al.*[5][22] for non-boiling steam-water flow system (p=10～109 atm), where $\langle\alpha_0\rangle$ is the measured value of the void fraction at $\langle j_l\rangle=0$.

(2) Correlation Procedure

In this section the exponents $n_1\sim n_5$ and the constant in Eq. (6) will be determined using the data of the present work and the available data in the literatures.

In **Fig. 9**, $\langle\alpha\rangle/\langle\alpha_0\rangle-1$ was plotted against $-\langle j_l\rangle/\langle j_g\rangle$ for various $\langle j_g\rangle$ and in **Fig. 10**

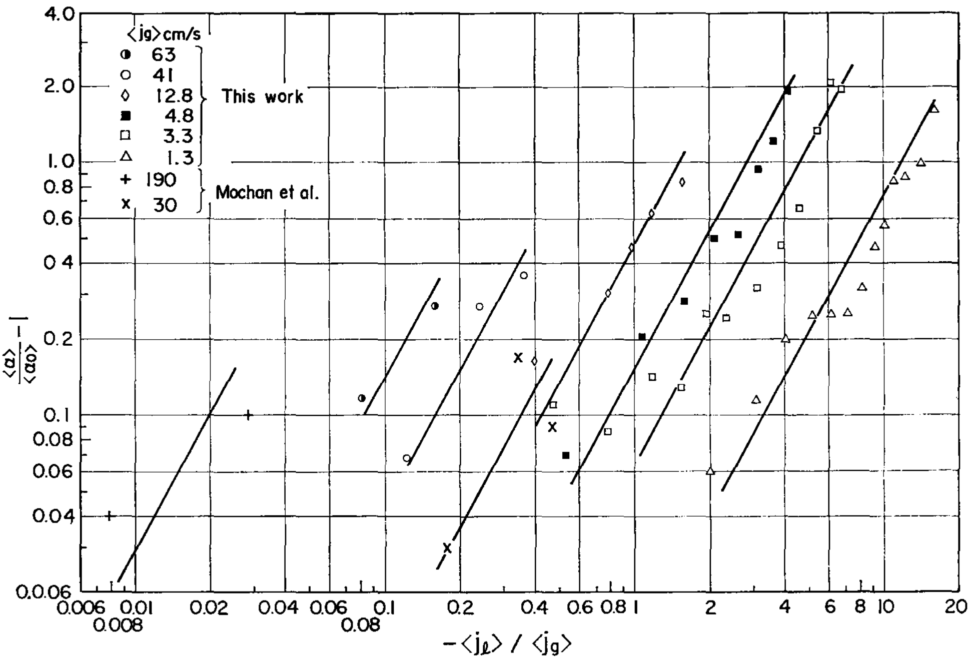

Fig. 9 $\langle\alpha\rangle/\langle\alpha_0\rangle-1$ *vs.* $-\langle j_l\rangle/\langle j_g\rangle$

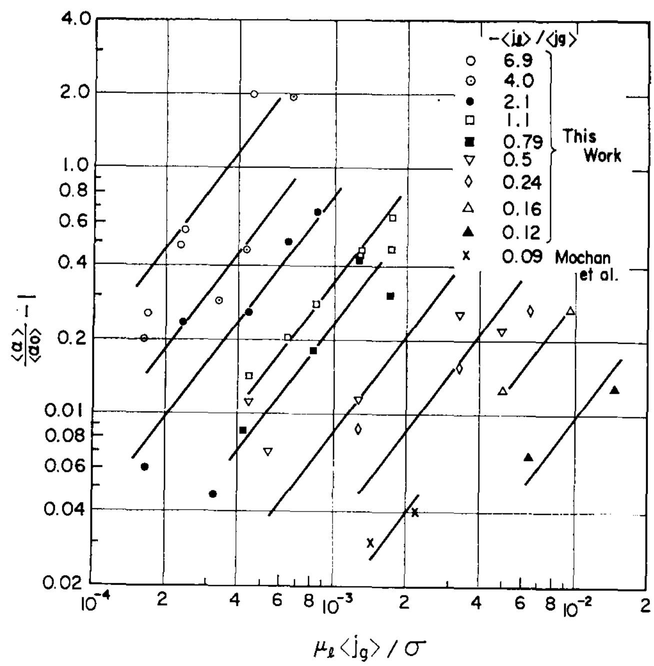

Fig. 10 $\langle\alpha\rangle/\langle\alpha_0\rangle-1$ *vs.* $\mu_l\langle j_g\rangle/\sigma$

is given the relation between the value of $\langle\alpha\rangle/\langle\alpha_0\rangle-1$ and $\mu_l\langle j_g\rangle/\sigma$ using $-\langle j_l\rangle/\langle j_g\rangle$ as a parameter for $D=40$ mm of the present data in air-water flow system. In these figures the data of Mochan *et al.*[22] for $D=76$ mm in steam-water flow system at pressure 10~12 atm are also plotted. From these data (including the present data of $D=80$ mm, not shown in the figures) linear correlation could be assumed for each parameter, for both air-water and steam-water flow systems and $n_5=1.8$ and $n_4=1.3$ were obtained with the data fit. Next, the effect of tube diameter on $\langle\alpha\rangle/\langle\alpha_0\rangle$ was investigated. To determine the effect **Fig. 11** was illustrated, which showed the present data of $D=40$ and 80 mm. The experimental results are plotted in terms of $\langle\alpha\rangle/\langle\alpha_0\rangle$ and dimensionless group $(\mu_l\langle j_g\rangle/\sigma)^{1.3}(-\langle j_l\rangle/\langle j_g\rangle)^{1.8}$, where the values of exponent 1.3 and 1.8 were obtained from above discussions. The results showed significant influence of tube diameter on $\langle\alpha\rangle/\langle\alpha_0\rangle$. It can

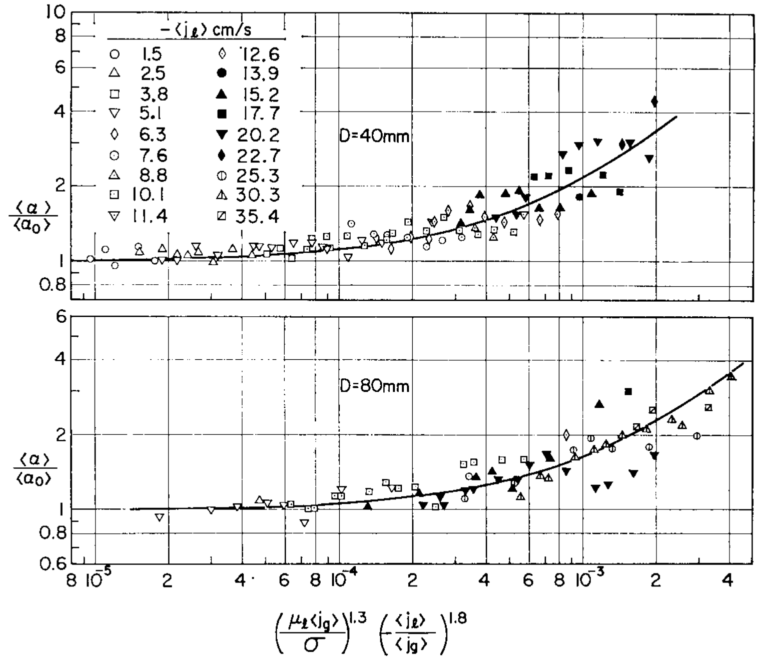

Fig. 11 Effect of diameter on $\langle \alpha \rangle / \langle \alpha_0 \rangle$

be seen that, as the $-\langle j_l \rangle$ values increase, the values of $\langle \alpha \rangle / \langle \alpha_0 \rangle$ increase; whereas for low values of $(\mu_l \langle j_g \rangle / \sigma)^{1.3} (-\langle j_l \rangle / \langle j_g \rangle)^{1.8}$, $\langle \alpha \rangle / \langle \alpha_0 \rangle$ tends to reach unity. The exponent n_3 of $\sqrt{\gamma_l D^2 / \sigma}$ was obtained as -0.9 with the data fit. The data of Bridge *et al.*[3] for air-water flow in 2 in. I. D. tube were also used to determine the value of n_3. The effect of physical properties on the value of exponent n_3 could not be checked because insufficient data were available to do so.

In order to investigate the effects of μ_g / μ_l and γ_g / γ_l, the experimental results reported by Bridge *et al.*[3] for air-58% glycerine solution flow and by Mochan *et al.*[5][22] for non-boiling steam-water flow in D=60 and 76 mm were plotted in **Fig. 12**. (Averaged value of the surface tension in the glycerine solutions was used to analyze the data.) For comparison purposes fitting curve for air-water systems has been drawn. If the determined relations

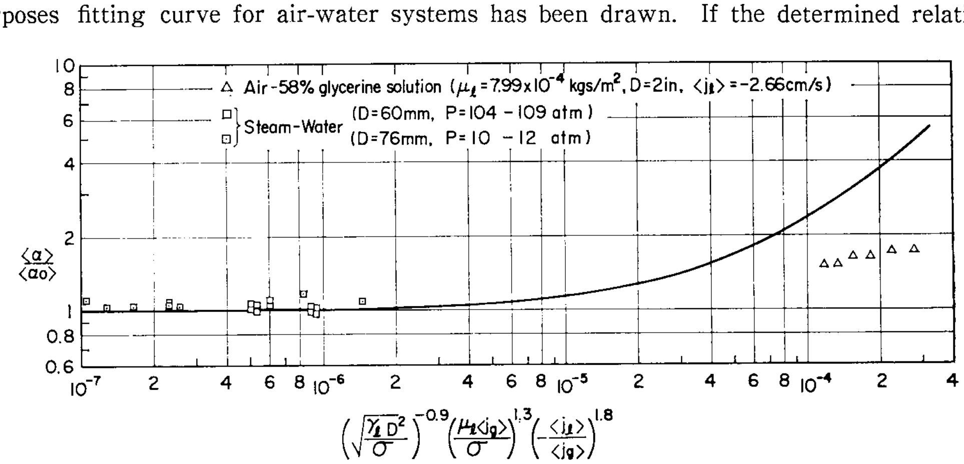

Fig. 12 Effect of fluid properties on $\langle \alpha \rangle / \langle \alpha_0 \rangle$

from both the data of air-water and steam-water flow systems were held for the data of air-58% glycerine solution flow system, deviations of the data from solid line could be explained by the effects of γ_g/γ_l and μ_g/μ_l. In fact, Sokolov *et al.*[25] reported that the difference of void fraction between air-water and air-glycerine solution flow systems for cocurrent flow is due to the influence of the properties of the fluid. Then it is found that increases in liquid viscosity and in pressure, that is in γ_l/γ_g, give a decrease in the values of $\langle\alpha\rangle/\langle\alpha_0\rangle$. The exponents n_1 and n_2, and the const. in Eq. (6) were determined as -0.4 and 0.7, and 1.6×10^4, respectively. As the result, the data of void fraction examined here for countercurrent gas-liquid two-phase flow in vertical tubes is correlated by

$$\langle\alpha\rangle/\langle\alpha_0\rangle=1+1.6\times10^4 z\,, \tag{7}$$

where $z=(\gamma_g/\gamma_l)^{-0.4}(\mu_g/\mu_l)^{0.7}(\sqrt{\gamma_l D^2/\sigma})^{-0.9}(\mu_l\langle j_g\rangle/\sigma)^{1.3}(-\langle j_l\rangle/\langle j_g\rangle)^{1.8}$.

Figure 13 shows that the final form of the correlation not depending on flow regime (solid line) and all the data used in compilating the correlation.

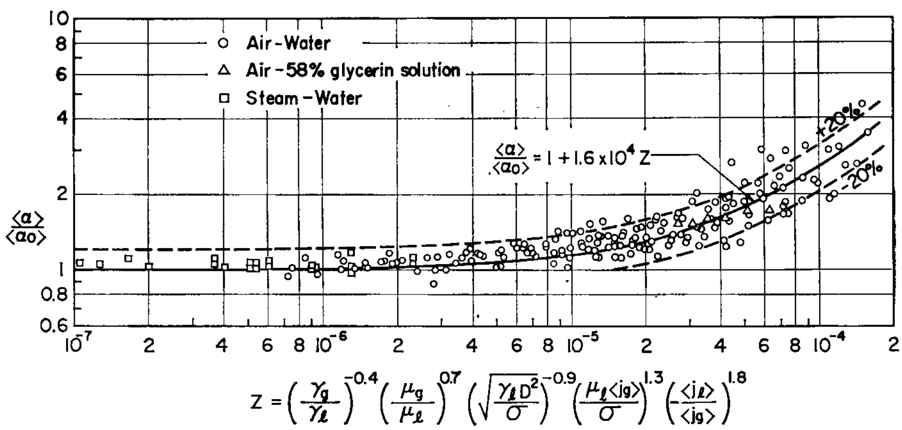

Fig. 13 Generalized correlation

The void fraction at stagnant water condition, $\langle\alpha_0\rangle$, may be obtained through the correlation developed by Wilson *et al.*[26] or Sudo[15].

Other forms of the correlation were tried, but a better prediction of the void fraction was obtained from the form of Eq. (6).

Additional experimental data are needed to clarify the effects of the physical properties and of the tube diameters on the void fraction as the experimental ranges examined in this study are limited.

V. Conclusions

The results of the present investigation may be summarized as follows:

(1) Experimental results on flow observations and the void fraction were presented for wide range of flow velocities of countercurrent air-water flow in vertical tubes.

(2) A correlation for predicting the void fraction of countercurrent gas-liquid flow in vertical tubes was developed, based on the dimensional analysis. The experimental ranges of the data used to develop the correlation are as follows: volumetric flux density of liquid 0∼−35.4 cm/s, volumetric flux density of gas 0.68∼115 cm/s, liquid

viscosity $0.94\times10^{-4}\sim7.99\times10^{-4}$ kgs/m^2, tube diameter 40~80 mm I.D. for two component flow system and volumetric flux density of water 0~−14 cm/s, volumetric flux density of steam 30~168 cm/s, pressure 10~109 atm, tube diameter 60~76 mm I.D. for one component flow system.

(3) The void fraction data were compared with the drift flux model for various flow patterns. For most flow patterns somewhat different results were obtained from previously published results for cocurrent flow.

[NOMENCLATURE]

C_0: Distribution parameter
D: Tube diameter
g: Acceleration due to gravity
$m_1\sim m_4$: Exponents in correlation (see Eq. (4))
$n_1\sim n_5$: Exponents in correlation (see Eq. (6))
j: Volumetric flux density
j_{gl}: Drift flux density
k: Exponent used in drift flux density (see Eq. (1))
V_{gj}: Drift velocity
α: Void fraction
γ: Specific weight
σ: Surface tension
μ: Viscosity
$\langle\ \rangle$: Average value over cross-sectional area of duct

(Subscripts)
0: at $\langle j_l\rangle=0$
g: Gas phase
l: Liquid phase

—REFERENCES—

(1) GRIFFITH, P., *et al.*: *AIChE paper* No. 25, Presented at 15th Nat. Heat Transfer Conf., San Francisco, Calif., 1975.
(2) SHULMAN, L.H., MOLSTAD, M.C.: *Ind. Eng. Chem.*, **42**[6], 1058 (1950).
(3) BRIDGE, A.G., *et al.*: *AIChE J.*, **10**[6], 819 (1964).
(4) FANTINI, L., *et al.*: *Energ. Nucl.* (*Milan*), **21**[1], 17 (1974).
(5) MOCHAN, S.I., *et al.*: *"Problems of Heat Transfer and Hydraulics of Two Phase Media"*, (KUTATELADZE, S.S. ed.), p. 304~326 (1969), Pergamon Press.
(6) SUGAWARA, S., *et al.*: *43th Western Japan Annu. Meeting, Japan Soc. Mech. Engrs.*, (in Japanese), 17 (1968).
(7) SERIZAWA, A.: Ph. D Thesis, Kyoto Univ., (1974).
(8) GRIFFITH, P., WALLIS, G.B.: *J. Heat Transfer*, **83**, 307 (1961).
(9) NICKLIN, O.J., *et al.*: *Trans. Inst. Chem. Engrs.*, **40**, 61 (1962).
(10) CURTET, R., DJONIN, K.: *Houille Blanche*, **5**, 531 (1967).
(11) MARTIN, C.S.: *J. Fluids Eng.*, **98**, 715 (1976).
(12) BLANDING, F.H., ELGIN, J.C.: *Trans. Am. Inst. Chem. Engrs.*, **38**, 305 (1942).
(13) WALLIS, G.B.: *Proc. Int. Heat Transfer Conf., ASME, Boulder, Colo.*, Vol. 2, Paper No. 38, p. 319~340 (1961).
(14) ZUBER, N., FINDLAY, J.A.: *J. Heat Transfer*, **87**, 453 (1965).
(15) SUDO, Y.: *J. Nucl. Sci. Technol.*, **17**[1], 1 (1980).
(16) WALLIS, G.B.: *"One-Dimensional Two-Phase Flow"*, (1969), McGraw Hill.
(17) GOLAN, L.P., STENNING, A.H.: *Proc. Instn. Mech. Engrs.*, 1969~70, **184** (Pt. 3C), 108 (1969).
(18) GRIFFITH, P.: *"Developments in Heat Transfer"*, (ROHSENOW, W.W. ed.), p. 274 (1964), MIT Press.
(19) HABERMAN, W.L., MORTON, R.K.: *DTMB*-802, (1953).
(20) MARTIN, C.S.: *"Flow Studies in Air and Water Pollution"*, ASME Symp. Atlanta, June, 1973, p. 49~60.
(21) DUMITRESCU, D.T.: *Z. Angew Math. Mech.*, **23**[3], 139 (1943).
(22) MOCHAN, S.I.: *E'nergomashinostr.*, **3**[5], 1 (1956).
(23) ZUBER, N., *et al.*: *GEAP*-5417, (1967).
(24) LORENZI, A., SOTGIA, G.: *Energ. Nucl.* (*Milan*), **23**[7], 396 (1976).
(25) SOKOLOV, V.N., *et al.*: *J. Appl. Chem. USSR*, (Z. PCH) **42**, Pt. 4, 814 (1969).
(26) WILSON, J.F., *et al.*: *Trans. Am. Nucl. Soc.*, **5**, 151 (1962).